Ccuf-921102--50

Performance of HT9 Clad Metallic Fuel at High Temperature*

ANL/FE/CP--76393

DE93 004852

by

R. G. Pahl, C. E. Lahm and S. L. Hayes

Fuels and Engineering Division
Argonne National Laboratory
Idaho Falls, Idaho 83403-2528

Paper submitted to the International Symposium
on Fuels for Liquid Metal Reactors
ANS/ENS 1992 International Conference

Chicago, Illinois
November 15-20, 1992

MASTER

DISTRIBUTION OF THIS DOCUMENT IS UNLIMITED

Performance of HT9 Clad Metallic Fuel
at High Temperature

R. G. Pahl, C. E. Lahm and S. L. Hayes*

1.0 Introduction

Steady-state testing of HT9 clad metallic fuel at high temperatures was initiated in EBR-II in November of 1987 [1,2]. At that time U-10 wt.% Zr fuel clad with the low-swelling ferritic/martensitic alloy HT9 was being considered as driver fuel options for both EBR-II and FFTF. The objective of the X447 test described here was to determine the lifetime of HT9 cladding when operated with metallic fuel at beginning of life inside wall temperatures approaching ~660°C. Though stress-temperature design limits for HT9 [3] preclude its use for high burnup applications under these conditions due to excessive thermal creep, the X447 test was carried out to obtain data on high temperature breach phenomena involving metallic fuel since little data existed in that area.

2.0 Test Description

The subassembly consisted of 19 HT9 clad and 30 D9 (a Ti-modified 316SS) clad 5.84-mm (0.230-in.) diameter fuel elements with 0.38-mm (0.015-in.) thick cladding and 1.07-mm (0.042-in.) diameter wire wrap. The remainder of the 61 positions in the bundle consisted of solid dummy elements added to reduce the mixed-mean sodium outlet temperature below the administratively imposed limit of 544°C.

The beginning-of-life inside wall temperatures ranged from ~630°C to ~660°C for the HT9 elements which were located in the center of the

* Argonne National Laboratory, P.O. Box 2528, Idaho Falls, ID, 83403-2528

hexagonal bundle and from ~525°C to ~620°C for the D9 elements. The fuel smeared densities were 75% and the peak core-midplane power was ~330 W/cm. The plenum-to-fuel volume ratio was ~1.5.

The X447 test was interrupted at 4.7 at. % burnup (284 equivalent full power days) for an interim examination which showed all elements intact and in good condition. The subassembly hardware was replaced and the test continued for an additional 335 equivalent full power days to a maximum burnup of 10.0 at. %. Eleven hours prior to the scheduled reactor shutdown, a fuel element breach was detected. An element breach was indicated by the presence of a xenon "tag" gas in the reactor cover gas. Mass spectroscopy analysis of specifically blended xenon isotopic ratios showed that the "tag" was one which had been injected into the plena prior to closure welding the X447 elements. A short-lived delayed neutron signal was associated with the breach event, coincident with increased fission gas concentrations. The spike was ~140 cps above the normal ~370 cps background in EBR-II, and lasted ~10 minutes which is typical for a metallic fuel breach [4]. Previous analysis showed that another breach had occurred ~30 days prior to the end of the run. The analysis of this "tag" was ambiguous, but X447's tag mixture was identified as a possible match. As described in detail in the subsequent section, two breached elements were eventually found in the X447 test, suggesting that the earlier breach had indeed occurred at approximately 9.5 at.% burnup. Simultaneous breaches of the two elements was ruled out because the total amount of xenon fission gas detected in the latter breach event was consistent with ~75% of the inventory of a single X447 element.

3.0 Post-Irradiation Examination Results

3.1 Unbreached Elements

At ~4.7 at.% burnup the cladding strain in the HT9 clad elements was negligible below x/L_0~0.70 (L_0 = original fuel column length of 34.3 cm). Typical peak diametral strains at top-of-core were approximately 0.8%. Because fuel-cladding mechanical interaction is weak at this smear density and burnup, and cladding irradiation swelling is nil, the localized strain

resulted from fission gas loading at this high temperature region of the element.

Fission gas analyses were performed on 4 unbreached elements after the test was terminated at 10 at.% burnup and the release fraction was found to range from 72% to 76% of theoretical production, typical for U-10Zr at ~10% burnup. Assuming an average gas temperature of 600°C, the pressure in-reactor would be ~7 MPa (~1015 psi) at 10 at.% burnup. Spiral contact profilometry measurements were made on all of the elements. The peak diametral strains ranged from 0.5% to 2.0% in the unbreached HT9 clad elements with maxima at top-of-core as expected for thermal creep dominated deformation. Failure strains in pressurized tube furnace tests are typically between 2% and 4% strain, indicating that few of the unbreached elements had significant margin to failure remaining at 10 at.% burnup. The D9 elements had peak strains ranging from 0.6% to 1.1% with maxima near the core-midplane as expected for swelling and irradiation creep dominated deformation.

3.2 Breached Elements

Post-irradiation element weights showed that two of the HT9 clad elements (DP70 and DP75) had lost 2.9 and 2.7 grams, respectively, typical for metallic fuel breaches when bond sodium and fission gas are expelled as the high pressure fission gas rushes out of the breach site. Neutron radiography indicated that the bond sodium was indeed absent in these two elements. This much weight loss represents a significant venting of fission gas and bond sodium since only ~0.9 grams of stable fission gas is produced at 10 at. % burnup and ~1.7 grams of bond sodium is loaded during manufacture. If one assumes 75% of the fission gas is located in the plenum and open fuel porosity, then 2.4 grams of weight loss can be accounted for if complete venting (and no fuel loss) occurred. The remaining weight loss (0.4 grams on the average) likely comes from the ~0.8 grams of fission product cesium. Cesium is insoluble in the fuel and is found as a liquid in isolated pores or alloyed with the bond sodium since they are completely soluble above 98°C, the melting point of sodium. Loss of cesium during breach is consistent with gamma-ray scans for the Cs-134

and Cs-137 isotopes, which showed that the intact elements had about twice the cesium activity in the fuel column as the breached elements.

Visual examination revealed sodium deposits on the cladding exterior at the top of the fuel column. However, after cleaning off the deposits, which presumably came from residual bond sodium oozing out of the breach , no cracks were visible at ~7X. Longitudinal irregularities were seen, which were later identified as necked regions associated with cracks. The two breached elements were adjacent to each other in the hexagonal bundle. The breach locations did not face each other. However, both breaches were located in the narrowest region of the coolant channel.. Figure 1 shows the general fuel structure in the region of the breach in element DP70.

Optical metallography showed that the breach occurred at the top of the fuel column in each element and corresponded to the regions of highest diametral cladding strain (4.0% in DP70 and 1.6% in DP75 including some necking strain). Figure 2 shows laser profilometry data (averaged 30° azimuthal scans) for the upper 1/5 of the fuel column for the breached elements and the hottest (per COBRA-WC code analysis) intact sibling element. Numerous cracks emanate from the cladding inner surface in the upper 4 cm of the breached elements. While no through cracks were intercepted by the serial grinding process, local necking was observed at the largest cracks which extended ~90% through the wall. Figure 3 shows a large crack and associated necking in element DP75. Optical metallography of the unbreached DP04 element showed less pronounced cracking, but narrow cracks of up to 20% of the wall were found associated with fuel/cladding chemical interaction (FCCI) discussed below.

Significant fuel cladding chemical interaction was observed in both breached elements and to a lesser extent in two unbreached siblings. The interaction was associated with two phenomena:
1) Brittle layers form in the cladding adjacent to the fuel that are rich in the lanthanide-series (rare earth) fission products. The layers are non uniform in depth around the perimeter of the fuel. Iron and nickel have diffused out of this band into the fuel. Lanthanide penetration on

grain boundaries ahead of the bulk layer is observed. Microhardness measurements showed the interaction layers to be very hard at ambient temperature (550 to 1080 DPH), and they contained numerous cracks. Transverse metallographic sections taken at ~6.4 mm intervals exposed penetration layers up to 45% of the wall thickness in breached elements and up to 20% of the wall in unbreached elements as shown in figure 4.

2) Soft layers of coarsened grains lacking the lath structure of the tempered martensite were also observed in the cladding. These regions extended up to 0.06 mm (0.0025 in.) deeper than the lanthanide layer. These layers are thought to be carbon depleted and were found in areas outboard of the lanthanide regions but also in regions where no lanthanide reaction had occurred. These layers were uncracked in the unbreached elements. In the case of breached elements, the soft layers had been penetrated by major cracks which had first penetrated the lanthanide layer.

4.0 Discussion

Having presented the phenomenology of the post-irradiation examination results from breached and intact elements tested at elevated cladding temperatures, the observed breach behavior can be discussed in the context of the issues raised regarding the operability of HT9 clad metallic fuel under these conditions. Given what is known about the creep properties of HT9, were the breaches at 10 at.% burnup unexpected? That is, to what extent did the large amounts of cladding penetration by lanthanide fission products and carbon depletion accelerate the time to failure? Given that the calculations of cladding temperatures are reliable, can the differences in lanthanide penetration between the breached and intact elements be explained?

4.1. Cumulative Damage Fraction (CDF) Calculations

The use of the cumulative damage or life fraction is a widely used method for predicting the lifetime of components subjected to creep damage at elevated temperatures. In this approach, it is assumed that the time to rupture t_r has previously been determined for constant stress σ

and constant temperature T conditions out of reactor. The fractional damage which occurs in time interval dt is simply dt/t_r. It is assumed that damage accumulates linearly so that rupture will occur when :

$$1 = \int_0^{t_f} \frac{dt}{t_r[\sigma(t), T(t)]}$$

In reality, due to the statistical uncertainty in the experiments used to obtain the stress rupture correlations and uncertainties in the in-reactor experiment itself, fuel element breach does occur at CDF values more or less than unity.

A number of CDF calculations were made in an attempt to determine if the breach in element DP70 could have been predicted. A beginning-of-life midwall temperature of 637 °C was calculated for the cladding at the breach site. The cladding temperature was assumed to decline ~0.06°C per full power day due to fuel burnup.

Estimates of the cladding stress history were made using the measured fission gas pressures and the plenum pressurization rate was assumed to be linear with time. Gas pressure loading was assumed to be the only source of stress. Nominal calculated temperatures were used but cladding wastage was conservatively applied from beginning-of-life. Using 0.076 mm (0.003 in.) of cladding wall thinning (the level of wastage observed in the intact elements) , the hoop stress at 10 at.% burnup reached ~68 MPa. The CDF for this case was ~0.007, indicating a very low probability of breach. HT9's creep rate in this temperature regime increases rapidly with temperature. For example, a 15°C increase in cladding temperature increased the calculated CDF to ~0.03, still a low probability of breach. Raising the midwall temperature 25°C increases the CDF to ~0.09, still a low failure probability but one which would generally be avoided by proper design or operating conditions.

If the maximum lanthanide penetration which was observed in the breached elements was applied, i.e. 0.17 mm (0.0067 in.), the calculated

hoop stress at 10% burnup increases to ~98 MPa. For the nominal temperature condition, the CDF at 10% burnup is ~0.06. Applying the 15°C temperature increase to this case raised the CDF to 0.3, while the 25°C increase raises the CDF to ~0.8. CDF values of 0.3 and 0.8 represent a significant probability of breach.

Since significant cladding wastage applied from beginning-of-life and temperatures somewhat above nominal were required to achieve CDF predictions representing a significant probability of failure, it appears that we have underpredicted stress rupture damage in our breached elements. However, plausible explanations for the apparent under-predictions of stress rupture damage can be made. The obvious ones would be a stress rupture correlation with large uncertainties in the temperature and stress regime of interest, temperature calculation errors (a bias toward cold temperatures), "hot spots" in the bundle, or fuel/cladding mechanical interaction forces that were ignored. However, irrespective of these effects, it appears that the fuel/cladding interaction has not been modeled in sufficient detail to judge the true nature of the discrepancies. Sharp cracks spanned the brittle lanthanide band in the cladding, even in an unbreached element. The unaffected cladding ligament is therefore subjected to stress-concentrators and would likely suffer a loss in lifetime compared to an unnotched sample subjected to the same thermal and pressure conditions. Second, the coarse-grained, carbon (or carbide) depleted zone outboard of the lanthanide zone may not be as creep resistant as the bulk HT9 it has replaced. The high temperature strength of HT9 depends on the size, number and spacing of the carbide precipitates, and it may be inappropriate to assume that the carbon depleted zone has strength equal to the non-depleted zone.

The CDF methodology for predicting breach in the X447 elements has met with limited success. More work is required to quantify the effects of crack initiators, carbide-depletion, and uncertainties in temperature calculations and ex-reactor stress rupture data.

7

4.2. The Effect of Breach on Fuel Temperatures

Approximately twice the lanthanide penetration was observed in the two breached elements than in the two intact elements. Breaches should occur in the elements with the highest cladding degradation assuming similar stress states, but temperature calculations show that the two breached elements are not significantly hotter than others in the X447 test. The peak beginning-of-life inside cladding temperatures for the four elements destructively examined were calculated as follows: DP04: 658°C, DP11: 654°C, DP70: 654°C, DP75: 639°C. Peak beginning-of-life fuel centerline temperatures are likewise not very different: DP04: 752°C, DP11: 747 °C, DP70: 746°C, and DP75: 730°C.

The thermal conductivity of metallic fuel is highest at beginning of life and decreases with burnup as the fuel swells and the fuel/cladding gap is redistributed as porosity in the bulk fuel. Significant pore interconnection is geometrically favored and experimental observations show that the bond sodium enters ("logs") the open porosity. This tends to improve the conductivity by offsetting somewhat the effects of the gas-filled pores.

As described in section 3.2, significant sodium loss took place after breach. Because logged sodium increases fuel thermal conductivity, it follows that expulsion of the sodium after breach can raise fuel temperatures. This can be expected to increase the migration rates of the lanthanides toward the cladding which in turn allows more FCCI to occur after breach. The magnitude of the effect would of course be dependent on the amount of time spent at full power in the breached condition.

To test this hypothesis, calculations were made of radial fuel temperature profiles as a function of the fraction of sodium logged for the conditions at or near the breach site in the X447 elements at 10% burnup. The fuel surface temperature was fixed at 677°C both before and after breach. The transverse metallography was used to construct a two-zone porosity model. The inner zone extended from $r/r_0 = 0$ to $r/r_0 = 0.33$ and

was assigned a porosity fraction of 50%. The outer zone was assigned a total porosity of 33%, yielding the overall porosity of 35%.

Because the exact amount of sodium logging is not known, bounding calculations were performed for the case where sodium filled all available pore space(B=1) and for the case of zero sodium logging (B=0) (figure 5). Two intermediate cases are also shown for 10% and 50% sodium logging (B=0.1 and B=0.5). Significant temperature increases can be expected whenever fuel with large amounts of logged sodium lose their sodium inventory. For any postulated mechanism of lanthanide transport, fuel temperature increase would tend to increase the kinetics of the process. One of the mechanisms for fission product transport in metallic fuel currently being investigated is vapor transport via interconnected porosity. This mechanism is based on the fact that a gradient in fission product vapor pressure from fuel centerline to fuel surface will cause vapor transport down the temperature gradient toward the cladding interface. The ratio of the difference in the vapor pressure at fuel centerline to that at fuel surface has been calculated for the cases of complete sodium venting (B=0) and complete sodium venting (B=1). For these extremes, the vapor pressure difference increases by the following factors: Nd:90, La:315, Ce:300, Pr:135, Sm:25 . Thus, at least for the case of vapor transport, enhanced lanthanide migration after breach is plausible since the driving force increases significantly with fuel temperature gradient.

The enhanced fuel cladding chemical interaction observed in the breached elements compared to unbreached siblings needs to be understood. Since the mechanism described above is strictly a post-breach phenomenon, it would be unnecessarily conservative to use the FCCI data from breached elements to derive a steady-state cladding wastage correlation. Comparisons of breached versus unbreached elements in other tests are needed to clarify this issue.

5.0 Conclusions

The following observations were made for the performance of high temperature metallic fuel irradiated in the X447 test.

1) Fifteen HT9 clad U-10Zr fuel elements were irradiated at peak cladding temperatures between ~630° and ~660°C, with two cladding failures occurring at ~9.5 at.% and 10.0 at.%.

2) The breach events were benign with regard to reactor operations.

3) Peak diametral strains in the intact HT9 clad elements ranged from ~0.5% to ~2.0%. The breached elements showed strains of ~1.6% and 4.0% which included some contribution from local necking.

4) Significant fuel/cladding chemical interaction was observed in the hottest cladding region. Lanthanide and cladding constituent interdiffusion resulted in brittle layers in the cladding which were prone to cracking in both the breached and intact elements examined. A soft grain-coarsened layer which may have been carbide-depleted was also observed beyond the lanthanide layer.

5) Cumulative damage fraction calculations indicated that the element lifetime was shorter than expected.

6) A possible mechanism for accelerated post-breach fuel/cladding chemical interaction was postulated based on fuel overheating due to sodium bond venting.

Acknowledgments

References

[1] R. G. Pahl, C. E. Lahm, H. Tsai and M. C. Billone, Proc. Int. Conf. on Fast Reactors and Related Fuel Cycles, Kyoto,1991, vol. III, P.1.19-1.

[2] R. G. Pahl, D. L. Porter, D.C. Crawford and L.C. Walters, J. of Nucl. Mater.,188 (1992) 3.

[3] G. L. Fox, Proc. of Int. Conf. on Reliable Fuels for Liquid Metal Reactors, Tucson, 1986, p5-135.

[4] R. G. Pahl, G. L. Batte', R. Mikaili, J. D. B. Lambert, and G. L. Hofman, Proc. Int. Conf. on Fast Reactors and Related Fuel Cycles, Kyoto,1991, vol. III, P.1.17-1.

<u>List of figure captions</u>:

Figure 1: Transverse optical metallography (as-polished) of the breach site in element DP70.

Figure 2: Cladding diametral profilometry profiles (30° azimuthal averages) for breached elements DP70 and DP75 and intact element DP04.

Figure 3: Transverse optical metallography of the breach site in element DP75 in the as-polished and etched conditions.

Figure 4: Penetration depth of the rare earth fission products in the HT9 cladding for two breached elements, DP70 and DP75, and intact elements DP04 and DP11.

Figure 5: Fuel temperature profiles for 10 at.% burnup at the breach site showing the effect of B, the fraction of pore volume which is logged with sodium.
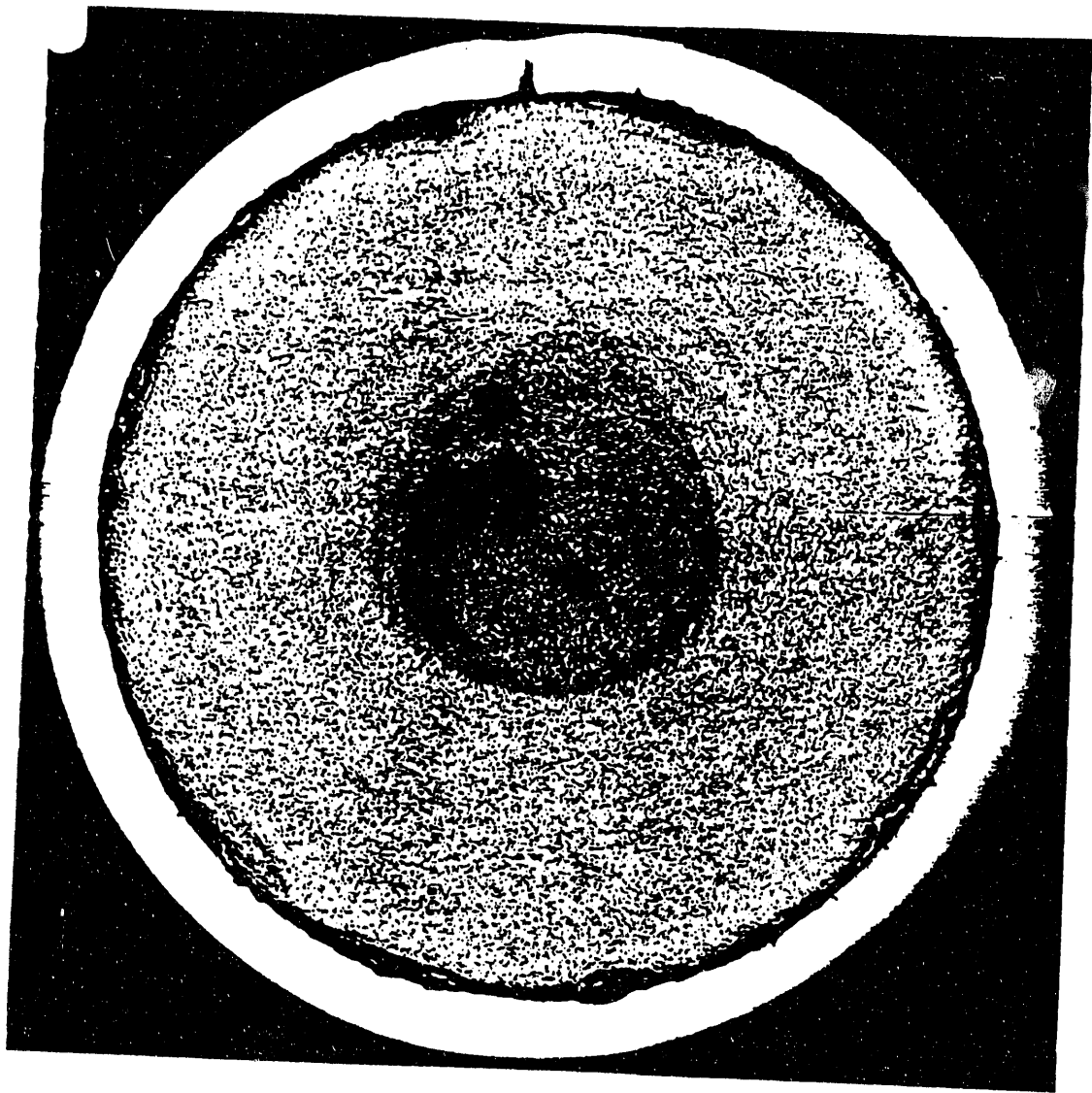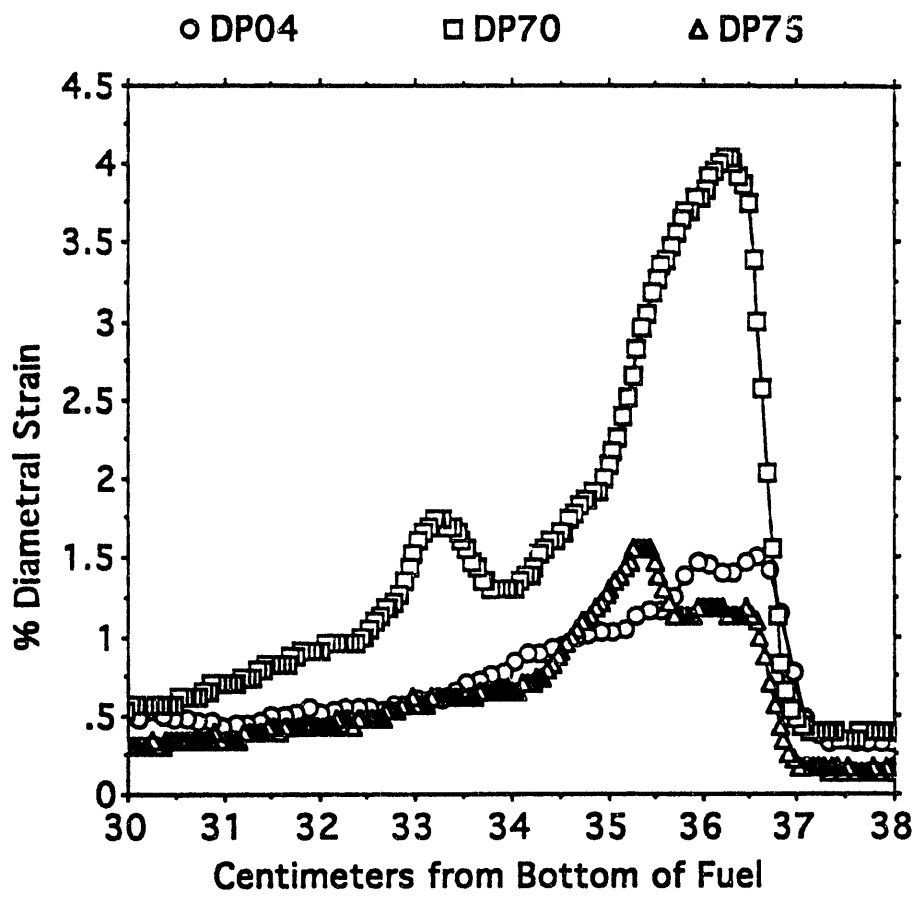
FIGURE 1.

Figure 2.

A major crack in the HT9 clad element DP75
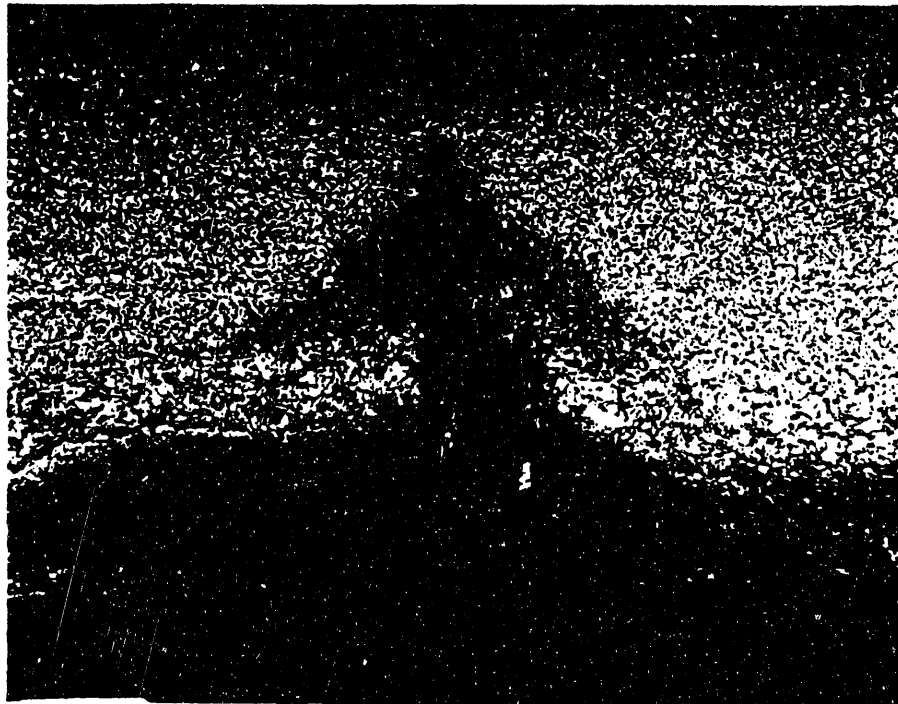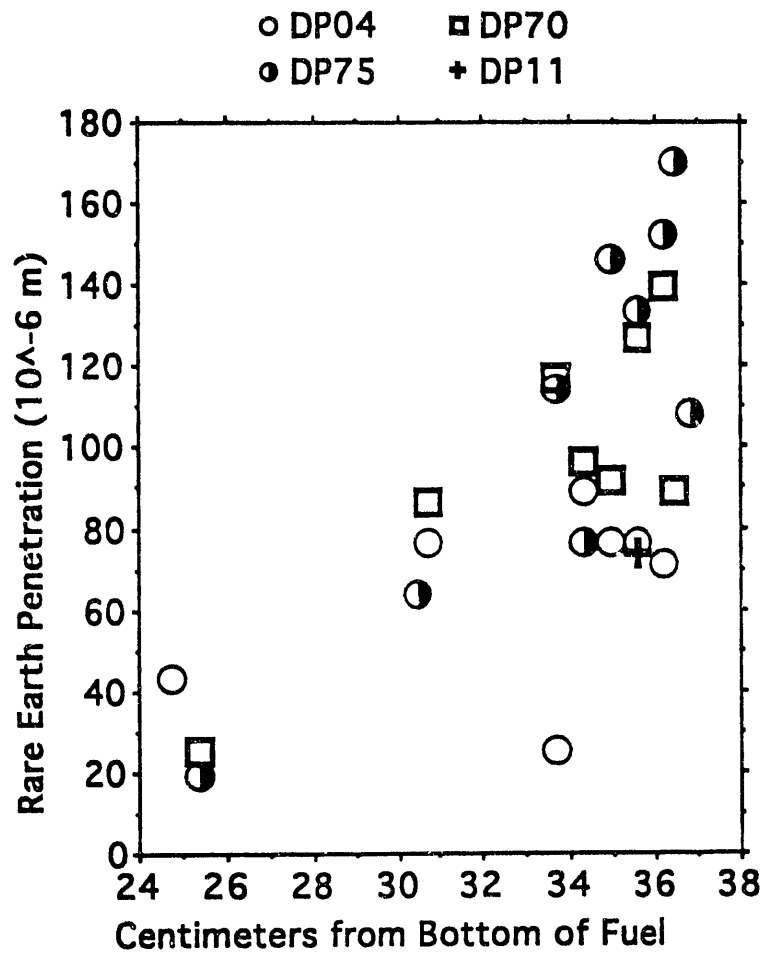(as-polished/ 20% NaOH electro-etched)

Figure 3.

Figure 4.

Figure 5.

END

DATE
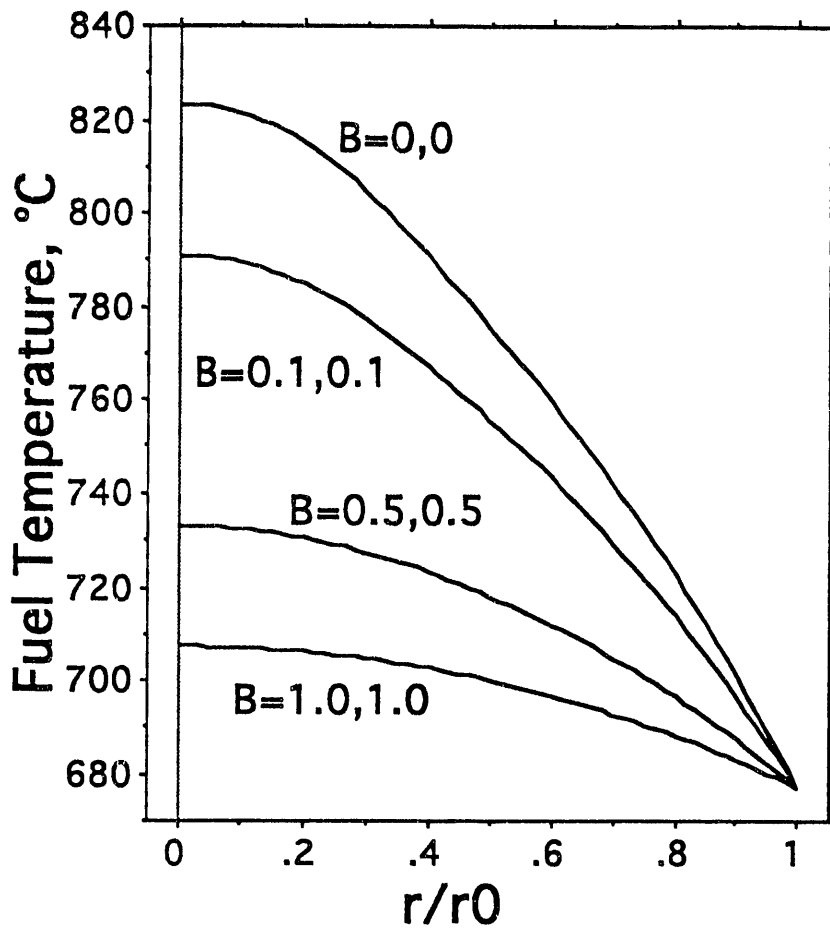## FILMED
5 / 4 / 93